Desalination and Water Treatment
www.deswater.com

doi: 10.5004/dwt.2017.21397

90 (2017) 241–251
September

Surface functionalization of D301 resin with urea: synthesis, characterization, and application for effective removal of toxic heavy metal ions

Fu-Qiang An*, Xiao-Yan Xue, Min Li, Tuo-Ping Hu, Jian-Feng Gao

Chemical Department, North University of China, Taiyuan 030051, China, Tel. 86-351-3923197; Fax: 86-351-3922118; emails: anfuqiang@nuc.edu.cn (F.-Q. An), 1056446066@qq.com (X.-Y. Xue), limin@126.com (M. Li), tuopinghu@126.com (T.-P. Hu), gaojianfeng@163.com (J.-F. Gao)

Received 12 May 2017; Accepted 29 August 2017

ABSTRACT

In this study, urea-modified D301 resin, UD301, was obtained successfully. The surface properties, chemical functional groups, element content, and surface morphology were investigated. The adsorption properties of UD301 for toxic heavy metal ions (Pb(II), Hg(II), Cd(II), and Ni(II)) were studied by batch method and the practical application value was evaluated by column method. The experimental results showed that UD301 possesses strong adsorption ability for Pb(II), Hg(II), Cd(II), and Ni(II). pH and temperature has a great influence on the adsorption capacity in the studied range. The adsorption capacities of UD301 towards Pb(II), Hg(II), Cd(II), and Ni(II) could reach 412.8, 396.9, 210.2, and 121.9 mg·g^{-1} at 293 K and pH of 6, respectively. The adsorption process was a typical monolayer chemical adsorption and could be well described by the Lagergren-first-order model. The adsorption was also an endothermic and spontaneous process drived by entropy. In addition, UD301 could be reused almost without any loss in the adsorption capacity.

Keywords: Adsorption; Removal; Heavy metal ions; Urea; D301 resin

1. Introduction

Heavy metal ions have been caused serious pollutants in surface waters and groundwater due to its high toxicity, poor biodegradability, and accumulation in the environment. Its accumulation in living bodies could cause serious diseases even at very low concentration. Pb(II), Hg(II), and Cd(II) are the most toxic metal ions for human. Ni(II) is usually existed in industrial wastewater, such as electroplating. Therefore, the effective removal of these heavy metal ions from water is very important and has attracted considerable research and practical interest. Numbers of methods or technologies, such as chemical precipitation [1,2], filtration [3,4], reverse osmosis [5], ion exchange [6–8] and adsorption [9–14], have been used to remove heavy metal ions from contaminated aqueous solutions. Among these methods or technologies, adsorption is still the most attractive and widely used method to remove low concentration of heavy metal ions from aqueous solutions because it is easy to handle, relatively cheap in cost, and effective in removing heavy metal ions even at low concentration. Compared with the activated carbons [9], zeolite [10], and other inorganic adsorbents [11], polymeric adsorbents or adsorption resins have a higher efficiency. For heavy metal ions, the amino-type adsorbents or resins possess strong adsorption ability by virtue of the coordination interaction between N atoms and metal ions [15–23].

D301 styrene macroporous weak basic resins are used widely to remove the toxic substance [24–26]. The adsorption force mainly comes from the coordination interaction between amino groups and metal ions and electrostatic interaction between protonated amino groups and anions. It is noticeable that the adsorption capacity is depended greatly on the number of action sites (mainly nitrogen-containing groups). Hence, the chemical modification with nitrogen-containing functional micromolecule or polymer is an effective approach to improve the adsorption abilities of existing adsorbent.

* Corresponding author.

Glycidyl methacrylate (GMA) is a commercial functional monomer, and possesses polymerizable double bond and high reactivity of epoxy group. Poly(glycidyl ethacrylate) (PGMA) can be grafted onto the surface of supporter via the polymerizable double bond and also be chemically modified with reagents containing amine group [27–29].

In this study, PGMA is grafted onto the surface of the D301 resin. Then, UD301 is obtained through ring-opening reactions between the epoxide rings of PGMA and the amino groups of urea. The adsorption abilities of UD301 for heavy metal ions are investigated.

2. Experiments

2.1. Materials and instruments

D301 styrene macroporous resin was purchased from Wandong Chemical Co., Ltd. (Anhui, China). GMA was purchased from Ruijinte Chemical Ltd. (Tianjin, China, AR grade) and purified by distillation under vacuum. Urea and other reagents were purchased from Beijing Chemical Plant (Beijing, China, AR grade).

Instruments used in this study were as follows: Agilent 5110 inductively coupled plasma (ICP) optical emission spectroscopy (Agilent Company, USA), S-4800 scanning electron microscope (SEM; Hitachi Company, Japan), Autosorb-iQ surface area analyzer (Quantachrome Company, USA), Perkin-Elmer 1700 infrared spectrometer (Perkin-Elmer Company, USA), Vario EL elemental analyzer (Elementar, Germany), PHS-3 acidimeter (Shanghai INESA Scientific Instrument Co., Ltd., China), and SHZ-C water-bathing constant temperature shaker (Shanghai Boxun Medical Biological Instrument Co., Ltd., China).

2.2. Preparation and characterizations of UD301

In total, 1 g of dry D301 resin and 10 mL of GMA were added into 100 mL of dimethyl formamide. Graft polymerization was initiated by ammonium persulfate (1.5 wt% of monomer) under N_2 atmosphere at 323 K for 18 h. The products were extracted with acetone in a Soxhlet apparatus to remove the polymers attaching physically onto the resins and then dried under vacuum. The resins were labeled as D301-*g*-PGMA. Subsequently, 1 g of D301-*g*-PGMA and 14 g of urea were added into 100 mL of sodium hydroxide aqueous solution with pH of 12. The ring-opening reaction between the amine groups of urea and the epoxide rings of PGMA was allowed to take place at 363 K for 8 h. Finally, the adsorbents were obtained after washing by distilled water and labeled as UD301. The preparation process is expressed in Fig. 1.

The SEM images of D301 and UD301 were measured to observe the change in surface morphologies before and after modification. The specific surface area (S_{BET}) was estimated by BET (Brunauer–Emmett–Teller) method. The total pore volume (V_{total}) was calculated from the liquid volume of N_2 at a relative pressure (p/p_0) of 0.99. The average pore diameter was obtained from S_{BET} and V_{total}. Fourier-transform infrared spectrum was measured by FTIR spectrometer using the conventional KBr pellet technique. The element content was measured by elemental analyzer.

2.3. Batch adsorption experiments

Batch adsorption experiments were performed using about 0.01 g of dry UD301 and 1,000 mL of metal ions solution. The concentration of metal ions was analyzed using

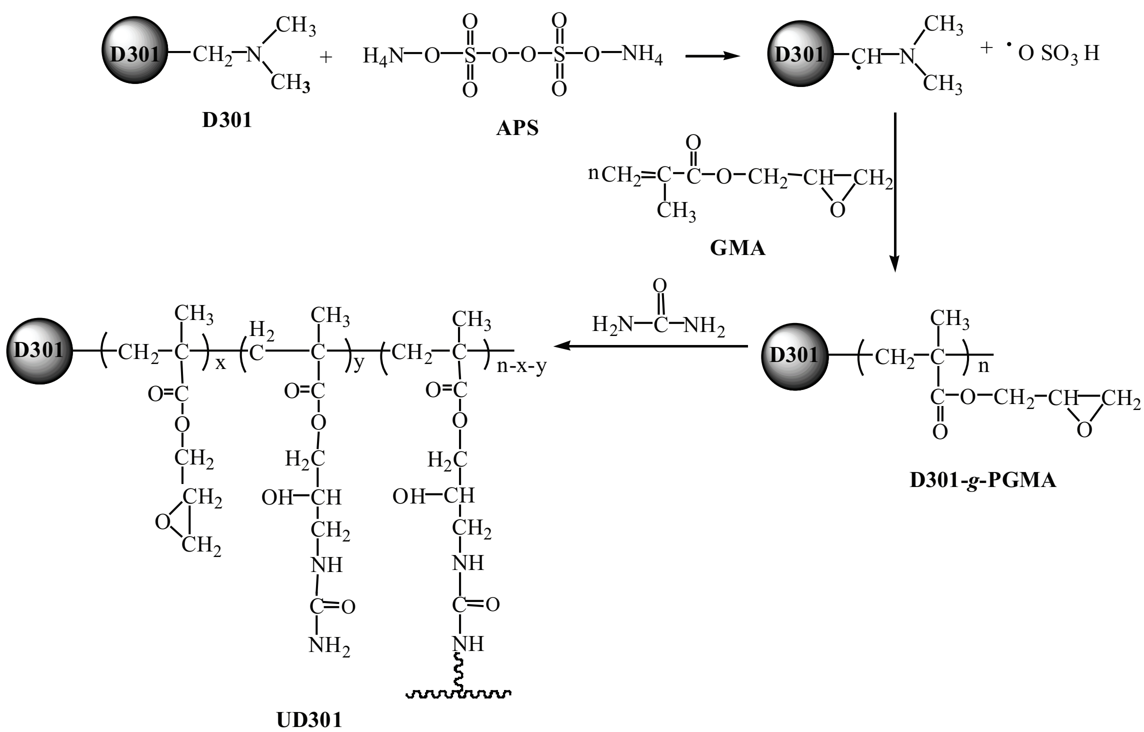

Fig. 1. Preparation process of UD301.

ICP optical emission spectrometer. The influences of contact time, initial concentration, pH of the solution, temperature, dosage of adsorbent, and concomitant metal ion on the adsorption capacity (Q, mg·g^{-1}) and adsorption efficiency (Aeff) were investigated. The adsorption capacity and adsorption efficiency were calculated according to the following equation:

$$Q = \frac{V(C_0 - C_t)}{m} \tag{1}$$

$$A_{\text{eff}} = \frac{C_0 - C_t}{C_0} \times 100\% \tag{2}$$

where V (L) is the volume of the solution, C_0 and C_t is the concentration of metal ions at start and t time in the solution (mg·L^{-1}), and m (g) is the weight of the adsorbent.

2.4. Column adsorption

In order to demonstrate further the practical application value of the UD301, the medium-scale experiment was also conducted by column method. The metal ion solution with the initial concentrations of 100 mg·L^{-1} was pass upstream through the column packaged with 1,014 g of UD301. The bed volume (BV) was 1 L and the flow rate was controlled at 0.2 L·min^{-1}. The effluent was collected and the concentration of metal ion was determined. The dynamics adsorption curve was plotted.

2.5. Repeated use experiment

Repeated usability (i.e., regenerability) was an important factor for an effective adsorbent. Desorption experiment was studied by batch experiment using the 1 mol·L^{-1} of nitric acid as eluent. The exhausted adsorbent was placed in the eluent and stirred continuously at 293 K for 1 h, and then the concentration of metal ions was analyzed using ICP optical emission spectrometer. In order to test the reusability of adsorption, the adsorption–desorption procedure was repeated 10 times.

3. Results and discussion

3.1. Characterizations

The SEM images of D301 and UD301 are shown in Fig. 2.

It can be seen that the surface of UD301 is rougher than that of D301. This may be resulted from the grafting modification of PGMA and urea.

The specific surface area (S_{BET}), total pore volume (V_{total}) and average pore diameter (d) of D301, D301-g-PGMA, and UD301 are listed in Table 1.

It can be seen that the specific surface area and total pore volume is small and the pore diameter is big comparing with

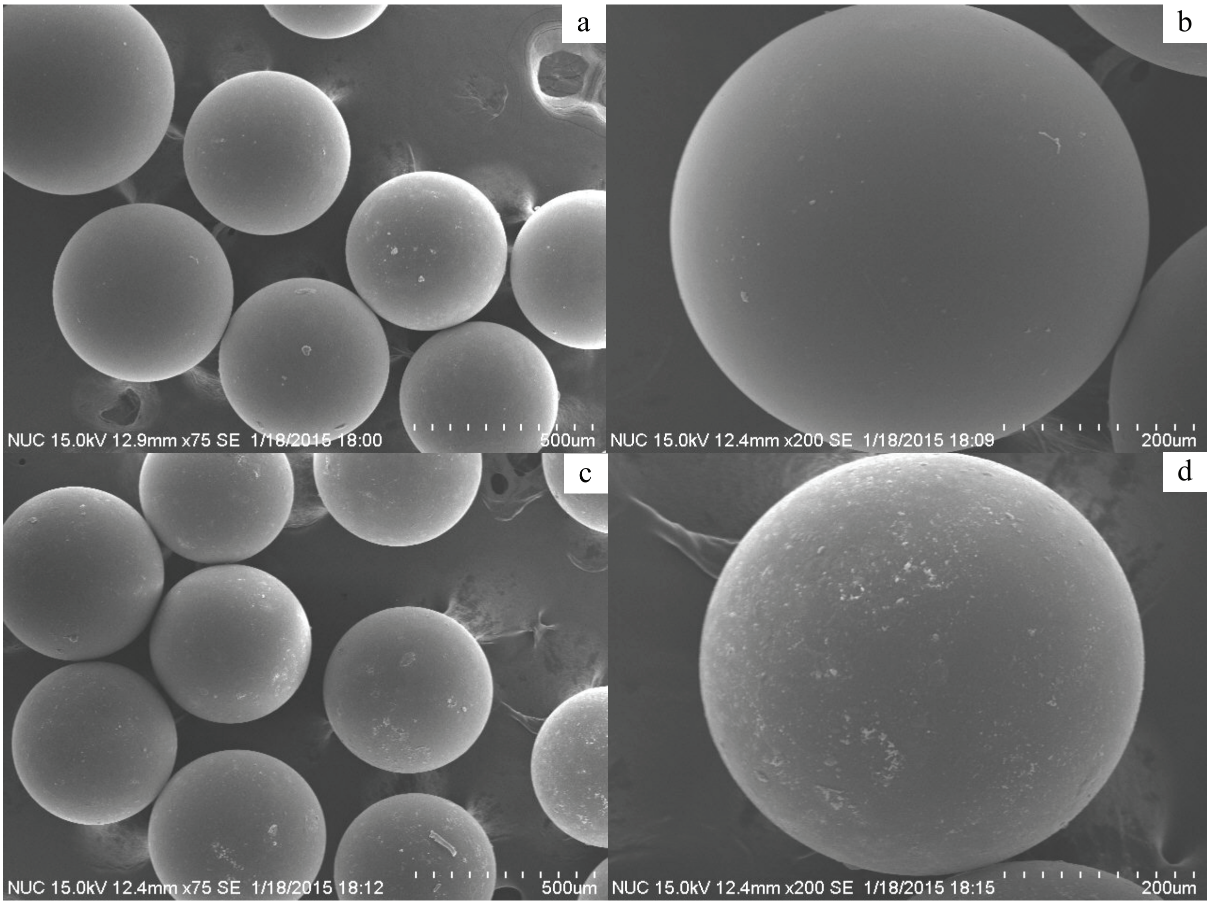

Fig. 2. The SEM images of D301 (a and b) and UD301 (c and d).

traditional porous adsorbents. This indicates that UD301 has not developed pore structure and it is impossible that UD301 form strong adsorption towards metal ions only depending on these underdeveloped pores.

The FTIR spectra of D301, D301-*g*-PGMA and UD301 are shown in Fig. 3. In the infrared spectrum of D301-*g*-PGMA, the characteristic absorptions of the epoxide rings and the carbonyl group appear at 1,143 and 1,743 cm^{-1}, respectively [27]. These indicate that PGMA macromolecules have been grafted onto the D301 resin surface and D301-*g*-PGMA has been formed.

In the infrared spectrum of UD301, the characteristic absorption of epoxide rings at 1,121 cm^{-1} is weaken greatly, the characteristic absorption of N–H bond at 3,445 cm^{-1} and the characteristic absorption of C=O bond at 1,720 cm^{-1} is enhanced. Combining the results of element analysis (Table 2), it could be attested that urea has reacted with the epoxide rings of PGMA, and UD301 is obtained. By virtue of the coordination interaction between N/O atoms and metal ions, the UD301 could adsorb metal ions effectively. The adsorption process and possible complexes between urea and metal ions according to other literature [30,31] are expressed in Fig. 4.

Table 1
The pore structure parameters of D301, D301-*g*-PGMA, and UD301

Samples	S_{BET} (m^2/g)	V_{total} (cm^3/g)	*d* (nm)
D301	202.3	0.059	121
D301-*g*-PGMA	197.6	0.052	113
UD301	195.4	0.050	111

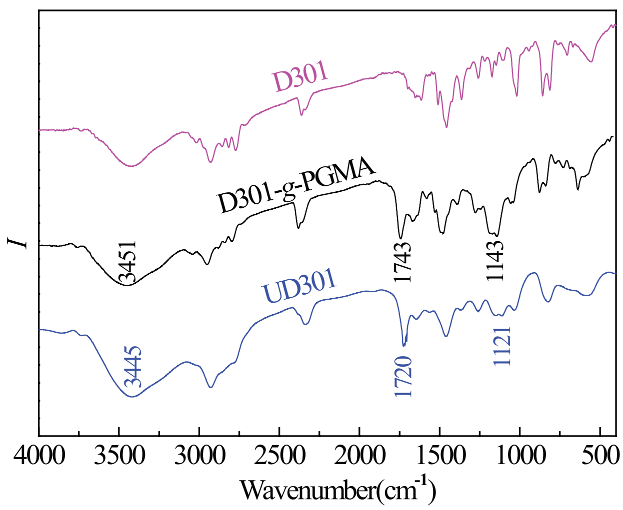

Fig. 3. FTIR spectra of D301, D301-*g*-PGMA, and UD301.

Table 2
Element analysis results

Samples	N (%)	C (%)	H (%)	O (%)
D301	6.13	69.93	8.73	14.94
D301-*g*-PGMA	3.56	65.40	8.02	23.02
UD301	9.92	58.95	7.85	23.28

3.2. Kinetic adsorption curve

The kinetic adsorption curves of UD301 towards Pb(II), Hg(II), Cd(II) and Ni(II) are shown in Fig. 5. It can be seen that UD301 possesses very strong adsorption ability towards Pb(II), Hg(II), Cd(II), and Ni(II) even at low initial concentration (10 mg·L^{-1}), and the saturated adsorption capacity of UD301 towards Pb(II), Hg(II), Cd(II), and Ni(II) is 412.8, 396.9, 210.2, and 121.9 mg·g^{-1} at 293 K and pH of 6, respectively. This can be attributed to the strong coordination interaction between N/O atoms and metal ions. The adsorption capacity of UD301 is higher than that of D301 resin and other adsorbents, and the comparisons are shown in Table 3.

In order to present the kinetic equation representing the adsorption behavior of metal ions onto UD301, the Lagergren-first-order model [46] and pseudo-second-order model [47] are used to test the experimental data. The fitting curves are also shown in Fig. 5 and the equations are shown as follows:

$$\ln(Q_e - Q_t) = \ln Q_e - k_1 t \quad (3)$$

$$t/Q_t = 1/(k_2 Q_e^2) + t/Q_e \quad (4)$$

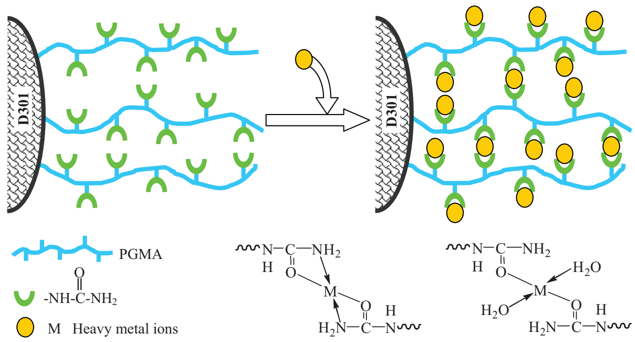

Fig. 4. Adsorption schematic illustration of UD301 towards heavy metal ions.

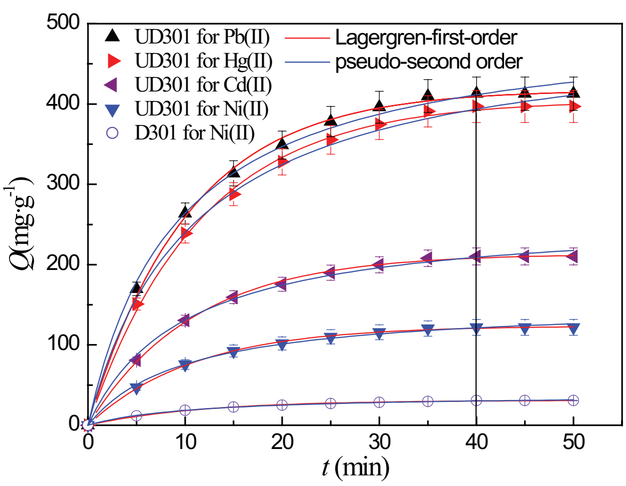

Fig. 5. Kinetic adsorption curves of D301 and UD301. Initial concentration: 10 mg·L^{-1}; weight of the adsorbent: 0.01 g; temperature: 293 K; pH: 6; repeated times: 5.

where Q_t (mg·g^{-1}) is the adsorption capacity at time t (min), Q_e (mg·g^{-1}) is the equilibrium adsorption capacity, k_1 (min^{-1}) and k_2 (g·mg^{-1}·min^{-1}) are the adsorption rate constant. The calculated equilibrium adsorption capacity, rate constant and the correlation coefficient (R^2) are summarized in Table 4.

Compared with the pseudo-second-order kinetic model, the R^2 of the Lagergren-first-order model is closer to 1.0 and the calculated equilibrium adsorption capacity is closer to the experimental data. This shows that the Lagergren-first-order model is more suitable to describe the adsorption process of metal ions onto UD301.

3.3. Adsorption isotherm

The adsorption isotherms of UD301 towards metal ions are shown in Fig. 6. In order to study the adsorption behavior of metal ions on UD301, the adsorption data are fitted by the Langmuir (Eq. 5), Freundlich (Eq. 6), and Sips (Eq. 7) equations. The fitting equations and their correlation

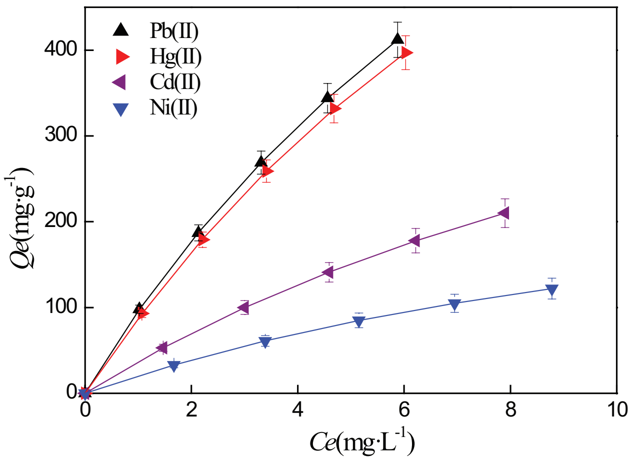

Fig. 6. Adsorption isotherms of UD301 towards metal ions. Temperature: 293 K; adsorption time: 40 min; pH: 6; repeated times: 5.

Table 3
The adsorption capacity of UD301 and other adsorbents

Adsorbents	T (K)	pH	Adsorption capacity (mg·g^{-1})				Reference
			Pb(II)	Hg(II)	Cd(II)	Ni(II)	
UD301	293	6	412.8	396.9	210.2	121.9	This study
M-PAM	298	4.5	20.3	–	27.99	7.28	[32]
M-PAM-HA	298	4.5	183.8	–	177.9	78.42	[32]
EGTA-chitosan	298	4	103.6	–	83.18	–	[33]
Activated carbon	298	9	–	330.9	183.2	–	[34]
Graphene oxide	303	7	–	–	93.8	62.3	[35]
SBA-15	333	6	43.5	–	53.1	42.3	[36]
Montmorillonite	298	4	54.3	–	22.9	–	[37]
Peanut husk powder	298	6	20	–	8	4.8	[38]
Bentonite	298	7	5.43	–	3.14	2.77	[39]
Fe_3O_4@EDTA	298	6	12	12	10	–	[40]
Graphitic-C_3N_4	298	5	281.8	–	112.4	37.6	[41]
UiO-66-NHC(S)NHMe	–	–	97	100	40	–	[42]
APTZ-PS	308	6	265	230	–	–	[43]
Hydrous ferric oxide	298	5	303.8	–	149.8	86.2	[44]
PEO/Chitosan	298	5	130	–	140	175	[45]

Table 4
The linear regression data of different models

Adsorption model	Metal ion	Q_e (mg·g^{-1})	Rate constant	R^2
Lagergren-first order	Pb(II)	417.7	0.097	0.9972
	Hg(II)	404.8	0.087	0.9974
	Cd(II)	213.4	0.092	0.9982
	Ni(II)	123.8	0.092	0.9983
Pseudo-second order	Pb(II)	505.1	2.2×10^{-4}	0.9921
	Hg(II)	500.0	1.9×10^{-4}	0.9923
	Cd(II)	261.1	3.9×10^{-4}	0.9922
	Ni(II)	151.3	6.7×10^{-4}	0.9934

Table 5
Adsorption regression equations and other coefficients of different equations

Model	Metal ion	Regression equation	R^2	R^2_{adc}
Langmuir	Pb(II)	$Q_e = 1289.8 \times 0.08 \times C_e/(1 + 0.08 \times C_e)$	0.9999	0.9994
	Hg(II)	$Q_e = 1334.8 \times 0.07 \times C_e/(1 + 0.07 \times C_e)$	0.9999	0.9992
	Cd(II)	$Q_e = 648.7 \times 0.061 \times C_e/(1 + 0.061 \times C_e)$	0.9999	0.9994
	Ni(II)	$Q_e = 328.8 \times 0.067 \times C_e/(1 + 0.067 \times C_e)$	0.9999	0.9993
Freundlich	Pb(II)	$Q_e = 102.5 \times C_e^{0.791}$	0.9982	0.9975
	Hg(II)	$Q_e = 94.28 \times C_e^{0.807}$	0.9976	0.9971
	Cd(II)	$Q_e = 41.76 \times C_e^{0.787}$	0.9977	0.9972
	Ni(II)	$Q_e = 24.14 \times C_e^{0.753}$	0.9965	0.9963
Sips	Pb(II)	$Q_e = 1391.3 \times 0.074 \times C_e^{0.98}/(1 + 0.074 \times C_e^{0.98})$	0.9999	0.9994
	Hg(II)	$Q_e = 1205.5 \times 0.078 \times C_e^{1.02}/(1 + 0.078 \times C_e^{1.02})$	0.9999	0.9994
	Cd(II)	$Q_e = 639.0 \times 0.061 \times C_e^{1.00}/(1 + 0.061 \times C_e^{1.00})$	0.9999	0.9995
	Ni(II)	$Q_e = 302.5 \times 0.072 \times C_e^{1.03}/(1 + 0.072 \times C_e^{1.03})$	0.9999	0.9994

coefficient (R^2) and adjusted determination coefficient (R_{adc}^2) are shown in Table 5.

$$Q_e = Q_0 K C_e/(1 + K C_e) \quad (5)$$

$$Q_e = k C_e^{1/n} \quad (6)$$

$$Q_e = Q_0 b C_e^m/(1 + b C_e^m) \quad (7)$$

where Q_e (mg·g^{-1}) is the equilibrium adsorption capacity, Q_0 (mg·g^{-1}) is the monolayer adsorption capacity, C_e (mg·L^{-1}) is the equilibrium concentration, K (L·mg^{-1}) is the Langmuir constant related to the adsorption energy, k is adsorption equilibrium constant that represents the strength of the adsorptive bond, n is the heterogeneity factor that represents the site energies distribution, b is the adsorption equilibrium constant, and m is the dissociation parameter. In Sips isotherm, if the value of b approaches 0, the Sips isotherm will become Freundlich isotherm. While the value of m = 1 or closer to 1, the Sips isotherm equation reduces to the Langmuir equation.

It can be seen that the R^2 and R^2_{adc} of Langmuir, Freundlich, and Sips isotherm are closer to 1. Furthermore, the value of m (0.98–1.03) of Sips equation is closer to 1, and the b of Sips equation is closer to the K of Langmuir equation. These imply that the adsorption of UD301 towards Pb(II), Hg(II), Cd(II), and Ni(II) is a Langmuir monolayer adsorption.

3.4. The influence of pH value on adsorption capacity

To avoid forming hydroxide precipitates, the adsorption is conducted at pH below 6. The adsorption performances of UD301 towards metal ions at different pH values are shown in Fig. 7.

The UD301 show a pH-dependent adsorption behavior. There is nearly no adsorption at the pH of 0, and the adsorption capacity increases significantly with the increase of the solution pH values before pH of 6. This phenomenon is similar to other amino adsorbent and can be explained from the adsorption driving force, coordination interaction between N/O atoms and metal ions. In strong acid environment, the excessive protons could enhance protonation degree of N atoms and produce competition effect on metal ions. This results in the weak coordination interaction and low adsorption capacity. With the increase of the solution pH, the protonation degree of N atoms is decreased and the coordination interaction is enhanced. Hence, the adsorption capacity increases with the increase of the solution pH.

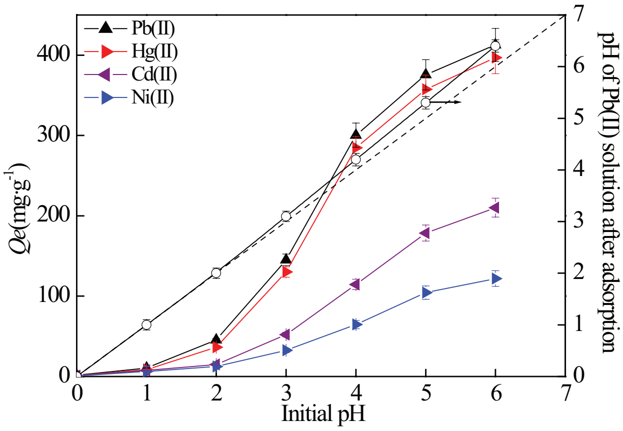

Fig. 7. The influence of pH on the adsorption capacity. Initial concentration: 10 mg·L^{-1}; temperature: 293 K; adsorption time: 40 min; repeated times: 5.

Additionally, low adsorption capacity at pH of 0 indicates that the exhausted adsorbent can be regenerated using strong acid as eluent.

3.5. The influence of temperature on adsorption capacity

Adsorption isothermal experiment under different temperature is conducted to determine the effect of temperature on the adsorption ability. The adsorption isotherms of UD301 towards metal ions under different temperature are shown in Fig. 8.

It can be seen that the adsorption capacities increase with the increase of the temperature, which demonstrates that the adsorption of UD301 towards metal ions is chemical adsorption.

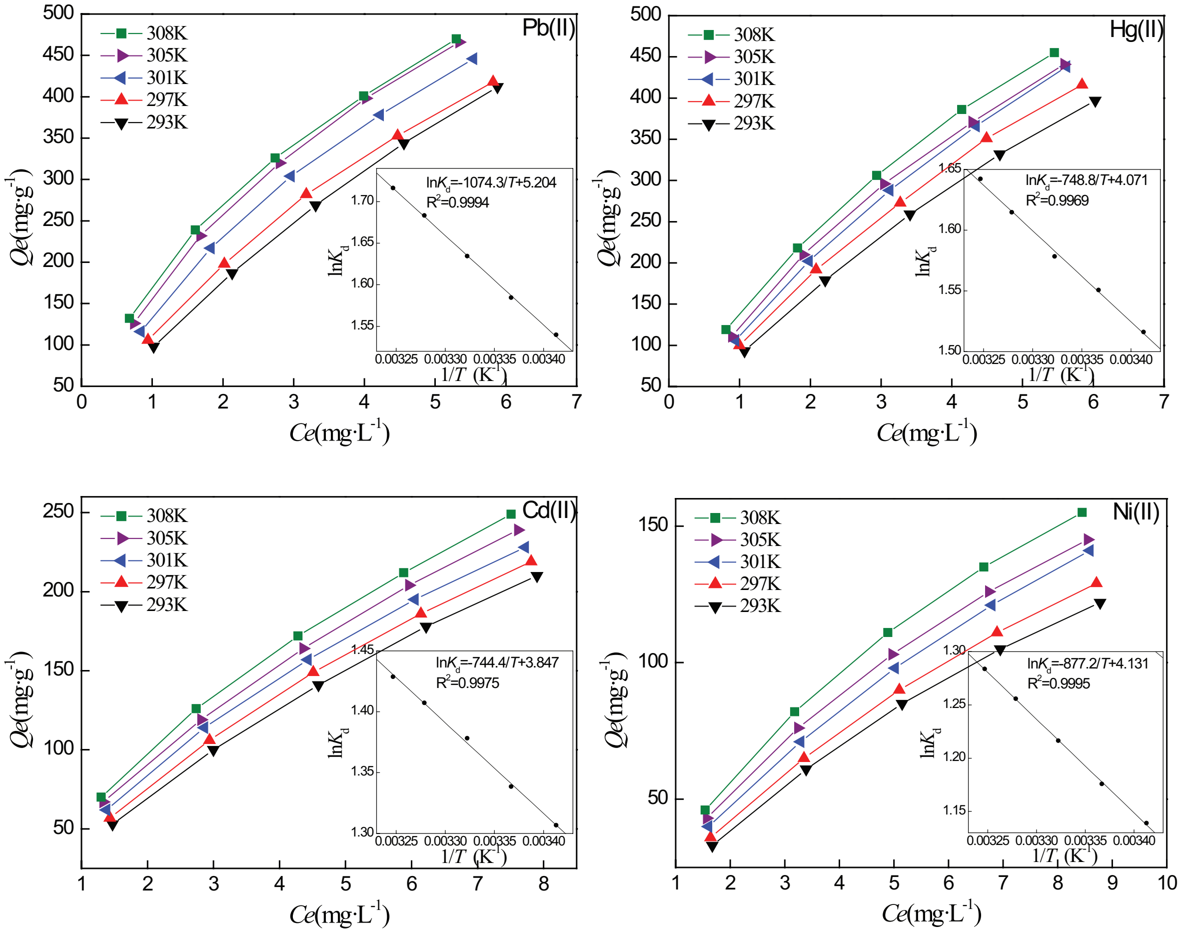

Fig. 8. Adsorption isotherms of UD301 towards metal ions under different temperature. Adsorption time: 40 min; pH = 6.

The thermodynamic equilibrium constant (K_d) is used to describe the equilibrium distribution of heavy metal ions between the solid and liquid phases and is equal to the intercept of $\ln(Q_e/C_e)$ versus Q_e according to Lyubchik et al. [48]. The Gibbs free energy change (ΔG) and entropy change (ΔS) at different temperatures and the enthalpy change (ΔH) are calculated according to the following equations, and all the thermodynamic parameters are listed in Table 6.

$$\Delta G = -\mathrm{RT}\ln K_d \tag{8}$$

$$\ln K_d = -\Delta H/\mathrm{RT} + C \tag{9}$$

$$\Delta G = \Delta H - T\Delta S \tag{10}$$

It can be seen that the values of ΔG for all metal ions are negative, which demonstrate that the adsorption process is spontaneous. The positive values of ΔH indicate that the adsorption process is endothermic and $\Delta H < T\Delta S$ indicates that the adsorption process is drived by entropy.

3.6. The influence of adsorbent dosage on adsorption efficiency

The influence of adsorbent dosage on adsorption efficiency (A_{eff}) is shown in Fig. 9. It can be seen that the adsorption efficiency increases with the increase of adsorbent dosage. The adsorption efficiency towards Pb(II), Hg(II), Cd(II), and Ni(II) could exceed 99.7% at the adsorbent dosage of 0.1 g. This indicates that UD301 can be used as adsorbents to remove heavy metal ions effectively even at low concentration.

3.7. The influence of concomitant metal ion on adsorption capacity

There are usually several kinds of metal cations present in real wastewater including Na(I), K(I), Mg(II) and Ca(II), which may lead to competitive adsorption against target metal ions. The adsorption capacity of UD301 towards Pb(II), Hg(II), Cd(II), and Ni(II) under different concentration of concomitant ions (1–10 mg·L^{-1}) is investigated using batch method. The results are listed in Table 7.

As it can be seen in Table 7 that the alkaline metal cation ions (Na(I) and K(I)) almost no suppressive effect on the adsorption of UD301 towards Pb(II), Hg(II), Cd(II) and Ni(II), while the adsorption capacity slightly decreased with increasing Mg(II) and Ca(II) concentration from 1 to 10 mg·L^{-1}. This is likely attributed to UD301 possessing stronger complexation ability with Pb(II), Hg(II), Cd(II), and Ni(II), and this can also indicate that UD301 could selectively adsorb heavy metal ions under the alkaline and alkaline earth metal ions background.

Table 6
Adsorption thermodynamic data of UD301 towards different ions

Metal ions	T (K)	K_d	ΔG (kJ·mol^{-1})	ΔH (kJ·mol^{-1})	ΔS (J·mol^{-1}·K^{-1})
Pb(II)	293	4.6663	–3.751	8.932	43.28
	297	4.8769	–3.913		43.25
	301	5.1268	–4.090		43.26
	305	5.3833	–4.268		43.28
	308	5.5644	–4.395		43.27
Hg(II)	293	4.5547	–3.693	6.226	43.09
	297	4.7194	–3.832		42.97
	301	4.8473	–3.950		42.80
	305	4.9910	–4.077		42.65
	308	5.1662	–4.205		42.65
Cd(II)	293	3.6943	–3.183	6.189	31.99
	297	3.8132	–3.305		31.97
	301	3.9676	–3.449		32.02
	305	4.0850	–3.569		31.99
	308	4.1732	–3.658		31.97
Ni(II)	293	3.1238	–2.775	7.293	34.36
	297	3.2407	–2.903		34.33
	301	3.3752	–3.044		34.34
	305	3.5109	–3.185		34.35
	308	3.6097	–3.287		34.35

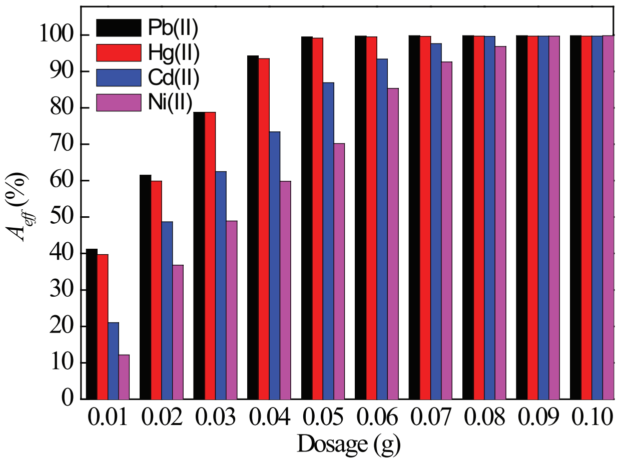

Fig. 9. The influence of adsorbent dosage on the adsorption efficiency. Initial concentration: 10 mg·L^{-1}; volume of the solution: 1,000 mL; temperature: 293 K; pH: 6.

3.8. Dynamic adsorption curve

In order to demonstrate further the practical application value of UD301, the metal ion solution (pH of 6, and the initial concentration of 100 mg·L^{-1}) was treated using UD301 column with upstream flows mode with the flow rate of 0.2 L·min^{-1}. The dynamic adsorption curve was shown in Fig. 10.

It can be seen that the leak of Pb(II), Hg(II), Cd(II), and Ni(II) appear at 4,176, 4,012, 2,173, and 1,238 BV, respectively. The metal ions were not detected almost by ICP in effluent before leak. This indicates that 1,014 g of UD301 could dispose effectively 4,176, 4,012, 2,173, and 1,238 L of Pb(II), Hg(II), Cd(II) and Ni(II) solution with initial concentration of 100 mg·L^{-1}, and the effluent reached completely the national sewage comprehensive emission standard (0.001 mg·L^{-1} of GB8978-1996).

3.9. Desorption and reusability

Good desorption performance and reusability of an adsorbent is important for its potential practical applications. In order to show the reusability of the UD301, the adsorption–desorption procedure is repeated 10 times, and the result is shown in Fig. 11. The result clearly shows that the UD301 could be used repeatedly without any lose in the significant adsorption capacity.

4. Conclusions

A new adsorbent, UD301, is obtained successfully based on the modification of D301 resin with urea. UD301 possess strong adsorption ability towards Pb(II), Hg(II), Cd(II), and Ni(II), and the adsorption ability is dependent greatly on the pH value and temperature in the studied range. The adsorption process could be well described by the Lagergren-first-order model and the adsorption of UD301 towards heavy metal ions is a typical monomolecular layer adsorption. The adsorption process is also an endothermic and spontaneous process drived by entropy. UD301 can be used to effectively remove the low concentrated heavy metal ions and could be reused almost without any loss in the adsorption capacity.

Table 7
The adsorption capacity of UD301 towards Pb(II), Hg(II), Cd(II) and Ni(II) under different concomitant ions

Concomitant ions	Concentration ($mg \cdot L^{-1}$)	Adsorption capacity ($mg \cdot g^{-1}$)			
		Pb(II)	Hg(II)	Cd(II)	Ni(II)
None	0	412.8	396.9	210.2	121.9
Na(I)	1	412.3	396.5	209.8	121.8
	5	412.1	396.2	209.4	122.1
	10	411.6	395.8	209.6	121.7
K(I)	1	412.5	396.4	209.9	121.6
	5	411.9	395.7	209.7	121.2
	10	412.1	396.2	209.6	121.7
Mg(II)	1	409.2	394.1	207.3	118.6
	5	408.6	393.8	207.4	118.3
	10	408.5	393.7	207.1	118.1
Ca(II)	1	408.9	394.3	207.6	118.6
	5	409.7	393.4	207.2	118.3
	10	408.3	393.2	207.4	118.5

Note: The concentration of Pb(II), Hg(II), Cd(II) and Ni(II) is 10 $mg \cdot L^{-1}$; The weight of the adsorbent is 0.01 g; temperature: 293 K; adsorption time: 40 min; pH: 6.

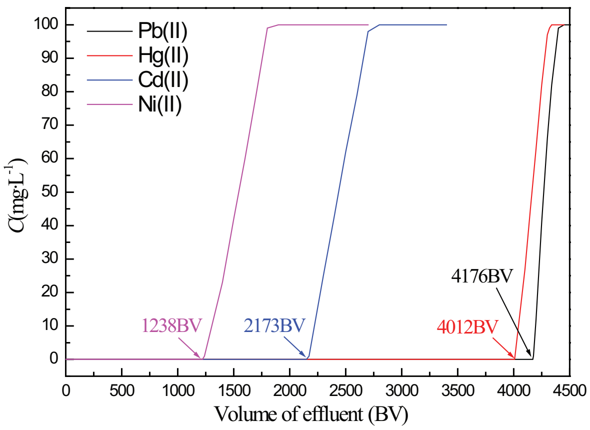

Fig. 10. Dynamic adsorption curve of UD301 towards metal ions. Temperature: 293 K; pH = 6; initial concentration: 100 $mg \cdot L^{-1}$.

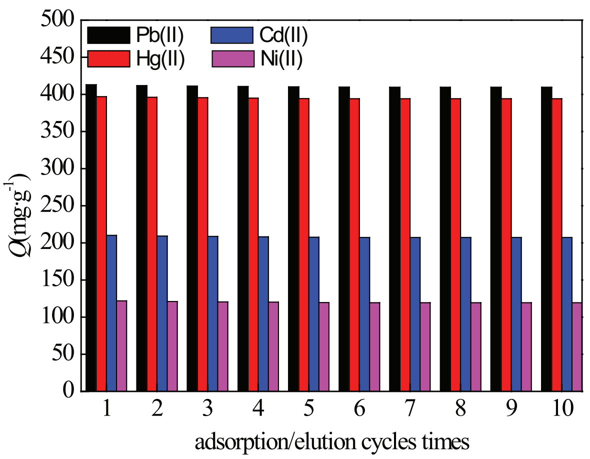

Fig. 11. Adsorption–desorption cycle of UD301.

Acknowledgments

The authors gratefully acknowledge the financial support of this work by the National Natural Science Foundation of China (21676258), International Science & Technology Cooperation Program of China (2011DFA51980), Shanxi Science & Technology Cooperation Program (2015081043), Natural Science Foundation of Shanxi Province (201601D102021), and Shanxi Province Key Laboratory of Higee-Oriented Chemical Engineering (CZL201501).

References

[1] G. Németh, L. Mlinárik, Á. Török, Adsorption and chemical precipitation of lead and zinc from contaminated solutions in porous rocks: possible application in environmental protection, J. Afr. Earth Sci., 122 (2016) 98–106.
[2] H. Sis, T. Uysal, Removal of heavy metal ions from aqueous medium using Kuluncak (Malatya) vermiculites and effect of precipitation on removal, Appl. Clay Sci., 95 (2014) 1–8.
[3] M.S. Islam, W.S. Choi, B. Nam, C. Yoon, H.J. Lee, Needle-like iron oxide@$CaCO_3$ adsorbents for ultrafast removal of anionic and cationic heavy metal ions, Chem. Eng. J., 307 (2017) 208–219.
[4] X. Fang, J. Li, X. Li, S. Pan, X. Zhang, X. Sun, J. Shen, W. Han, L. Wang, Internal pore decoration with polydopamine nanoparticle on polymeric ultrafiltration membrane for enhanced heavy metal removal, Chem. Eng. J., 314 (2017) 38–49.
[5] Y.C. Xu, Z.X. Wang, X.Q. Cheng, Y.C. Xiao, L. Shao, Positively charged nanofiltration membranes via economically mussel-substance-simulated co-deposition for textile wastewater treatment, Chem. Eng. J., 303 (2016) 555–564.
[6] P. Kumar, A. Pournara, K.H. Kim, V. Bansal, S. Rapti, M.J. Manos, Metal-organic frameworks: challenges and opportunities for ion-exchange/sorption applications, Prog. Mater. Sci., 86 (2017) 25–74.
[7] T.M. Zewail, N.S. Yousef, Kinetic study of heavy metal ions removal by ion exchange in batch conical air spouted bed, Alex. Eng. J., 54 (2015) 83–90.
[8] H.X. Chang, Q. Fu, Y. Huang, A. Xia, Q. Liao, X. Zhu, Y.P. Zheng, C.H. Sun, An annular photobioreactor with ion-exchange-membrane for non-touch microalgae cultivation with wastewater, Bioresour. Technol., 219 (2016) 668–676.

[9] S. Jiang, L. Huang, T.A.H. Nguyen, Y.S. Ok, V. Rudolph, H. Yang, D. Zhang, Copper and zinc adsorption by softwood and hardwood biochars under elevated sulphate-induced salinity and acidic pH conditions, Chemosphere, 142 (2016) 64–71.

[10] U. Habiba, A.M. Afifi, A. Salleh, B.C. Ang, Chitosan/(polyvinyl alcohol)/zeolite electrospun composite nanofibrous membrane for adsorption of Cr^{6+}, Fe^{3+} and Ni^{2+}, J. Hazard. Mater., 322 (2017) 182–194.

[11] H.C. Vu, A.D. Dwivedi, T.T. Le, S.H. Seo, E.J. Kim, Y.S. Chang, Magnetite graphene oxide encapsulated in alginate beads for enhanced adsorption of Cr(VI) and As(V) from aqueous solutions: role of crosslinking metal cations in pH control, Chem. Eng. J., 307 (2017) 220–229.

[12] M. Ferhat, S. Kadouche, N. Drouiche, K. Messaoudi, B. Messaoudi, H. Lounici, Competitive adsorption of toxic metals on bentonite and use of chitosan as flocculent coagulant to speed up the settling of generated clay suspensions, Chemosphere, 165 (2016) 87–93.

[13] H. Ge, T. Hua, X. Chen, Selective adsorption of lead on grafted and crosslinked chitosan nanoparticles prepared by using Pb^{2+} as template, J. Hazard. Mater., 308 (2016) 225–232.

[14] Y. Qi, J. Wang, X. Wang, J.J. Cheng, Z. Wen, Selective adsorption of Pb(II) from aqueous solution using porous biosilica extracted from marine diatom biomass: properties and mechanism, Appl. Surf. Sci., 396 (2017) 965–977.

[15] V. Hernández-Morales, R. Nava, Y.J. Acosta-Silva, S.A. Macías-Sánchez, J.J. Pérez-Bueno, B. Pawelec, Adsorption of lead (II) on SBA-15 mesoporous molecular sieve functionalized with $–NH_2$ groups, Micropor. Mesopor. Mat., 160 (2012) 133–142.

[16] C. McManamon, A.M. Burke, J.D. Holmes, M.A. Morris, Amine-functionalised SBA-15 of tailored pore size for heavy metal adsorption, J. Colloid Interf. Sci., 369 (2012) 330–337.

[17] X. Xin, Q. Wei, J. Yang, L. Yan, R. Feng, G. Chen, B. Du, H. Li, Highly efficient removal of heavy metal ions by amine-functionalized mesoporous Fe_3O_4 nanoparticles, Chem. Eng. J., 184 (2012) 132–140.

[18] N. Velikova, Y. Vueva, Y. Ivanova, I. Salvado, M. Fernandes, P. Vassileva, R. Georgieva, A. Detcheva, Synthesis and characterization of sol-gel mesoporous organosilic as functionalized with amine groups, J. Non-Cryst. Solids, 378 (2013) 89–95.

[19] T.S. Anirudhan, S. Jalajamony, S.S. Sreekumari, Adsorption of heavy metal ions from aqueous solutions by amine and carboxylate functionalised bentonites, Appl. Clay Sci., 65–66 (2012) 67–71.

[20] X. Zhang, Q. Huang, M. Liu, J. Tian, G. Zeng, Z. Li, K. Wang, Q. Zhang, Q. Wan, F. Deng, Y. Wei, Preparation of amine functionalized carbon nanotubes via abioinspired strategy and their application in Cu^{2+} removal, Appl. Surf. Sci., 343 (2015) 19–27.

[21] M. Hadavifar, N. Bahramifar, H. Younesi, M. Rastakhiz, Q. Li, J. Yu, E. Eftekhari, Removal of mercury(II) and cadmium(II) ions from synthetic wastewater by a newly synthesized amino and thiolated multi-walled carbon nanotubes, J. Taiwan Inst. Chem. E., 67 (2016) 397–405.

[22] X. Guo, B. Du, Q. Wei, J. Yang, L. Hu, L. Yan, W. Xu, Synthesis of amino functionalized magnetic graphenes composite material and its application to remove Cr(VI), Pb(II), Hg(II), Cd(II) and Ni(II) from contaminated water, J. Hazard. Mater., 278 (2014) 211–220.

[23] C. Fan, K. Li, J. Li, D. Ying, Y. Wang, J. Jia, Comparative and competitive adsorption of Pb(II) and Cu(II) using tetraethylenepentamine modified chitosan/$CoFe_2O_4$ particles, J. Hazard. Mater., 326 (2017) 211–220.

[24] T. Shi, Z. Wang, Y. Liu, S. Jia, C. Du, Removal of hexavalent chromium from aqueous solutions by D301, D314 and D354 anion-exchange resins, J. Hazard. Mater., 161 (2009) 900–906.

[25] J. Zhang, X. Liu, X. Chen, J. Li, Z. Zhao, Separation of tungsten and molybdenum using macroporous resin: competitive adsorption kinetics in binary system, Hydrometallurgy, 144–145 (2014) 77–85.

[26] G. Xiao, R. Wen, Comparative adsorption of glyphosate from aqueous solution by 2-aminopyridine modified polystyrene resin, D301 resin and 330 resin: influencing factors, salinity resistance and mechanism, Fluid Phase Equilibr., 411 (2016) 1–6.

[27] F.Q. An, B.J. Gao, X. Dai, M. Dai, X.H. Wang, Efficient removal of heavy metal ions from aqueous solution using salicylic acid type chelate adsorbent, J. Hazard. Mater., 192 (2011) 956–962.

[28] A. Gupta, R. Jain, D.C. Gupta, Studies on uptake behavior of Hg(II) and Pb(II) by amine modified glycidyl methacrylate-styrene-N,N′-methylenebisacrylamide terpolymer, React. Funct. Poly., 93 (2015) 22–29.

[29] Y. Fu, J. Wu, H. Zhou, G. Jin, Removal of nickel(II) from aqueous solutions using iminodiacetic acid functionalized polyglycidyl methacrylate grafted-carbon fibers, Chinese J. Chem. Eng., 23 (2015) 919–923.

[30] D. Gangopadhyay, S.K. Singh, P. Sharma, H. Mishra, V.K. Unnikrishnan, B. Singh, R.K. Singh, Spectroscopic and structural study of the newly synthesized heteroligand complex of copper with creatinine and urea, Spectrochim. Acta A., 154 (2016) 200–206.

[31] X. Wu, S. Zhang, Q. Niu, T. Li, A novel urea-derived fluorescent sensor for highly selective and sensitive detection of Fe^{3+}, Tetrahedron Lett., 57 (2016) 3407–3411.

[32] F. Zhao, W.Z. Tang, D. Zhao, Y. Meng, D. Yin, M. Sillanpää, Adsorption kinetics, isotherms and mechanisms of Cd(II), Pb(II), Co(II) and Ni(II) by a modified magnetic polyacrylamide microcomposite adsorbent, J. Water Process Eng., 4 (2014) 47–57.

[33] F. Zhao, E. Repo, D. Yin, M.E.T. Sillanpää, Adsorption of Cd(II) and Pb(II) by a novel EGTA-modified chitosan material: kinetics and isotherms, J. Colloid Interf. Sci., 409 (2013) 174–182.

[34] P.G. González, Y.B. Pliego-Cuervo, Adsorption of Cd(II), Hg(II) and Zn(II) from aqueous solution using mesoporous activated carbon produced from *Bambusa vulgaris* striata, Chem. Eng. Res. Des., 92 (2014) 2715–2724.

[35] P. Tan, J. Sun, Y. Hu, Z. Fang, Q. Bi, Y. Chen, J. Cheng, Adsorption of Cu^{2+}, Cd^{2+} and Ni^{2+} from aqueous single metal solutions on graphene oxide membranes, J. Hazard. Mater., 297 (2015) 251–260.

[36] E. Da'na, A. Sayari, Adsorption of heavy metals on amine-functionalized SBA-15 prepared by co-condensation: applications to real water samples, Desalination, 285 (2012) 62–67.

[37] C. Chen, H. Liu, T. Chen, D. Chen, R.L. Frost, An insight into the removal of Pb(II), Cu(II), Co(II), Cd(II), Zn(II), Ag(I), Hg(I), Cr(VI) by Na(I)-montmorillonite and Ca(II)-montmorillonite, Appl. Clay Sci., 118 (2015) 239–247.

[38] I. Abdelfattah, A.A. Ismail, F.A. Sayed, A. Almedolab, K.M. Aboelghait, Biosorption of heavy metals ions in real industrial wastewater using peanut husk as efficient and cost effective adsorbent, Environ. Nanotechnol. Monit. Manage., 6 (2016) 176–183.

[39] A.A. Taha, M.A. Shreadah, A.M. Ahmed, H.F. Heiba, Multi-component adsorption of Pb(II), Cd(II), and Ni(II) onto Egyptian Na-activated bentonite: equilibrium, kinetics, thermodynamics, and application for seawater desalination, J. Environ. Chem. Eng., 4 (2016) 1166–1180.

[40] E. Ghasemi, A. Heydari, M. Sillanpää, Superparamagnetic Fe_3O_4@EDTA nanoparticles as an efficient adsorbent for simultaneous removal of Ag(I), Hg(II), Mn(II), Zn(II), Pb(II) and Cd(II) from water and soil environmental samples, Microchem. J., 131 (2017) 51–56.

[41] C. Shen, C. Chen, T. Wen, Z. Zhao, X. Wang, A. Xu, Superior adsorption capacity of $g\text{-}C_3N_4$ for heavy metal ions from aqueous solutions, J. Colloid Interf. Sci., 456 (2015) 7–14.

[42] H. Saleem, U. Rafique, R.P. Davies, Investigations on post-synthetically modified UiO-66-NH_2 for the adsorptive removal of heavy metal ions from aqueous solution, Micropor. Mesopor. Mater., 221 (2016) 238–244.

[43] Y. Zhang, Y. Chen, C. Wang, Y. Wei. Immobilization of 5-aminopyridine-2-tetrazole on cross-linked polystyrene for the preparation of a new adsorbent to remove heavy metal ions from aqueous solution, J. Hazard. Mater., 276 (2014) 129–137.

[44] Y. Zhang, Z. Li, Heavy metals removal using hydrogel-supported nanosized hydrous ferric oxide: synthesis, characterization, and mechanism, Sci. Total. Environ., 580 (2016) 776–786.

[45] M. Aliabadi, M. Irani, J. Ismaeili, H. Piri, M.J. Parnian, Electrospun nanofiber membrane of PEO/chitosan for the adsorption of nickel, cadmium, lead and copper ions from aqueous solution, Chem. Eng. J., 220 (2013) 237–243.
[46] S. Lagergren, About the theory of so-called adsorption of soluble substances, Zur theorie der sogenannten adsorption gelöster stoffe, K. Svenska Vetensk Akad. Handl., 24 (1898) 1–39.
[47] Y.S. Ho, G. McKay, Pseudo-second order model for sorption processes, Process Biochem., 34 (1999) 451–465.
[48] S.I. Lyubchik, A.I. Lyubchik, O.L. Galushko, L.P. Tikhonova, J. Vital, I.M. Fonseca, S.B. Lyubchik, Kinetics and thermodynamics of the Cr (III) adsorption on the activated carbon from comingled wastes, Colloids Surf. A Physicochem. Eng. Asp., 242 (2004) 151–158.